



High Throughput Tip-Less Electrospinning via a Circular Cylindrical Electrode

Dezhi Wu¹, Xiaoping Huang¹, Xiting Lai¹, Daoheng Sun^{1,*}, and Liwei Lin^{2,*}

¹Department of Mechanical and Electrical Engineering, Xiamen University,
Xiamen 361005, P. R. China

²Department of Mechanical Engineering, Berkeley Sensor & Actuator Center,
University of California, Berkeley, California 94720, USA

High throughput production of nanofibers by means of “Tip-less Electrospinning” (TLES) has been demonstrated using a circular cylinder as the emitting electrode. Electrohydrodynamics instabilities on a thin liquid film under high electrical field can generate artificial liquid jets for the TLES process. Experimental results have shown that the yield of poly(ethylene oxide) nanofibers can be more than 260 times in weight as compared with a single-jet electrospinning process. Parameters affecting the TLES process including applied voltage, polymer solution concentration, electrode-to-substrate distance and the thickness of liquid films have been characterized. As such, TLES has potential for high-throughput, massive production of electrospun nanofibers.

Keywords: Electrohydrodynamics, Nanofiber, Polymer, Tip-Less Electrospinning.

1. INTRODUCTION

The superior characteristics of nanofibers such as high surface area to volume ratio and specific properties (optical, mechanical, electrical and chemical) have led to several promising applications, including filtration,¹ scaffolds for tissue engineering,² wound dressing and protective clothing,³ reinforced composite materials,⁴ and micro/nano sensors and actuators.⁵ The ability to fabricate nanofibers from a broad range of polymeric materials with controllability has greatly accelerated in recent years with advancement in electrospinning processes, such as aligned arrays and orderly patterns.^{6–9} However, high production speed of electrospun nanofibers has been a key technology challenge. Previously, multiple-jet setup has been the main approach to speed up the manufacturing processes. For example, three different arrangements of multi-electrode array (line-shape, elliptical and concentric mode) have been studied and it was concluded that concentric electrospinning setup has provided the best efficiency and quality of electrospun nanofibers.¹⁰ The influence of different applied voltages on electrodes has also been investigated. It was found that fiber quality decreased under higher applied bias voltages as the electric fields from individual electrode interfered with each other.¹¹ In another approach, a cylindrical, shell-shape electrode was introduced with the

setup of multiple electrodes to stabilize the electrospinning process with better uniformity.¹²

In the tip-less electrospinning demonstrations, there have been two recent reports. First, ferromagnetic fluid was used under a magnetic field with the addition of an electrical field. This setup generates steady vertical spikes and results in upward jetting of nanofibers.¹³ Second, a porous tube was used with random holes of 10–100 μm in diameters. It was shown to generate numerous jets under high applied voltages and suitable air pressure to supply liquid polymer through the pores.¹⁴ Nanofibers were deposited on the inner surface of a cylindrical collector that enclosed the porous cylindrical tube.

This paper presents results in a tip-less electrospinning setup using a circular cylindrical surface as the electrode. In contrast to the previously published reports, there are no needle arrays, no ferromagnetic liquid layer and no porous tube in this setup. The mechanism is based on electrohydrodynamics (EHD) induced fluctuations on top of relatively smooth surface to create artificial liquid jets for electrospinning. Furthermore, unlike conventional tip-based electrospinning processes, the common problem of clogging on the syringe tip is eliminated.

2. EXPERIMENTAL DETAILS

The setup of the high throughput tip-less electrospinning consists of four components as illustrated in

*Authors to whom correspondence should be addressed.

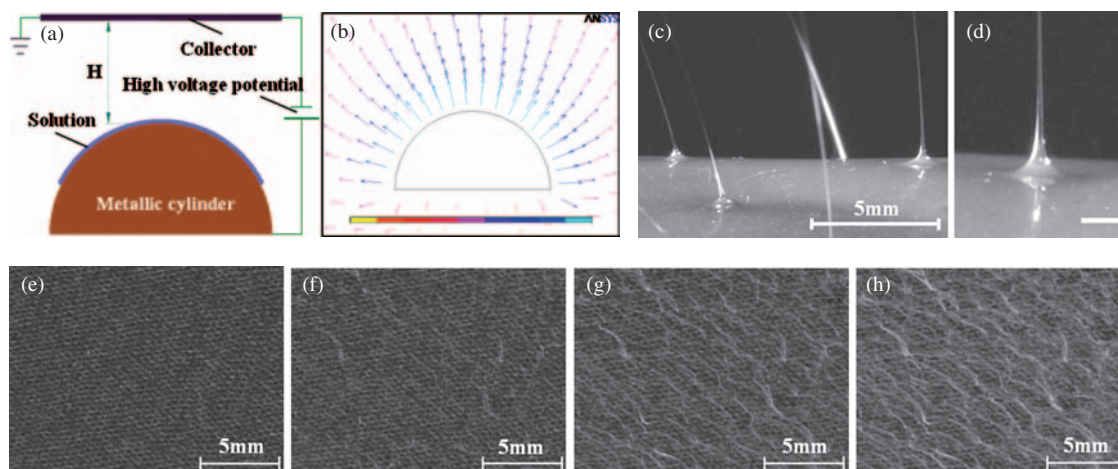


Fig. 1. (a) Schematic diagram of TLES. (b) Electric field simulation using ANSYS. The electrode distance, applied voltage and the diameter of the cylinder are 15 cm, 50 kV and 3 cm respectively. (c) Experimental results showing multi-jets under applied voltage of 60 kV. The electrode-to-collector distance is 15 cm and the diameter of the cylindrical electrode is 5 cm. (d) Close view showing a single jet and its base. Scale bar: 1 mm. (e)–(h) Photos of nanofibers collected on the black fabric after 20, 40, 60 and 80 seconds of TLES.

Figure 1(a): a cylindrical-shape electrode, a scraper, a ground collector and a high voltage supplier. Circular cylinders made of either stainless steel or copper have been successfully used as the tip-less electrode with different surface roughness of RA numbers (arithmetic average deviation from the center line of the surface) of 1.6 and 6.3, respectively. Cylinders with different diameters (1–6 cm) and 12 cm in length have been tested. The scraper is used to control the thickness of the deposited polymer solution. A high voltage power supply with operating voltage ranging from 0 to 120 kV and resolution of 0.1 kV is used. The flat ground collector is made of copper meshes and is covered with black woven cloth to collect electrospun nanofibers which are emitting upwards against the gravity force as illustrated.

Poly(ethylene oxide) (PEO) and water/ethanol mixture have been used as the polymer solution in this preliminary work. The typical concentration of PEO ($M_v = 300,000$) solution used is from 12 wt% to 20 wt%. The solvent is composed of 80 wt% deionized water and 20 wt% ethanol. Ethanol is used to increase the evaporation rate in order to facilitate solidification of nanofibers.¹⁵ The polymer solution is placed on the surface of the cylindrical cylinder to form a 0.5 to 2 mm thick liquid layer by using the plastic scraper.

In our experiments, it is found that flat-shape emitting electrodes are much more difficult to initiate the electrospinning process as compared with cylindrical-shape electrodes. Computer simulation in Figure 1(b) shows that under an applied bias voltage of 50 kV, electrode-to-substrate distance of 15 cm and cylindrical electrode diameter of 3 cm, the highest electrical field reaches $9.3 \times 10^5 \text{ V} \cdot \text{m}^{-1}$ at the top edge of the electrode. On the other hand, the flat-shape electrode under the same condition only generates an average electrical field at about $3.9 \times 10^5 \text{ V} \cdot \text{m}^{-1}$.

It is found that high polymer solution concentration results in large diameters of nanofibers and similar phenomena have been reported in conventional electrospinning processes.¹⁶ Experimentally, several liquid jets are

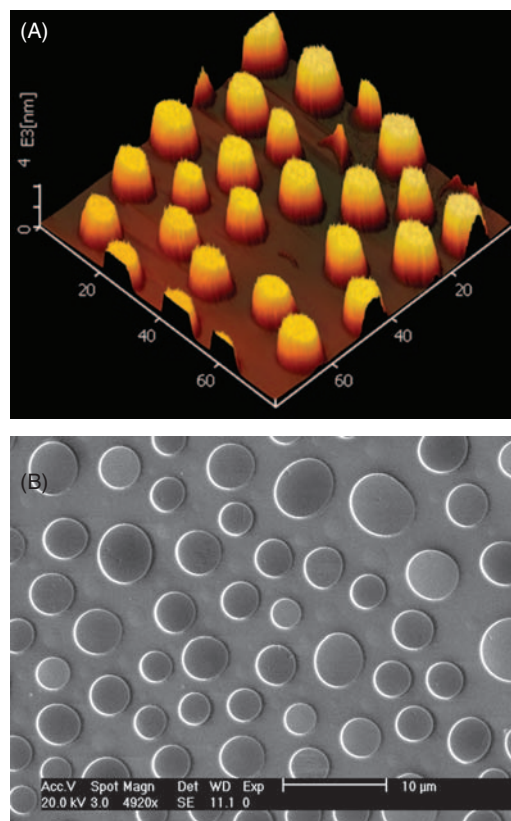


Fig. 2. (A) AFM of photoresist 1805 pillars on silicon substrate. Initial thickness: 1.1 μm ; electrode gap: 4 μm ; (B) SEM of photoresist 1805 pillars. Initial thickness: 432 nm; electrode gap: 1.1 μm . The applied voltage and the ambient temperature are 160 V and 171° respectively.

generated during the process as shown in Figure 1(c), where the scale bar is 5 mm. The typical number of liquid jets is about 3–4 per cm^2 and the effective electrospinning width in this case is about 3.3 cm (the cylinder is 3 cm in diameter). Therefore, the 12 cm-long cylindrical electrode used in this work can generate one hundred jets during the electrospinning process for high throughput nanofiber production. Figure 1(d) is the close view of a single jet. It is observed that the typical Taylor cone shape is formed during the electrospinning process.¹⁷ Figure 1(e)–(h) shows experimental results of electrospun fibers on a black cloth after collection time of 20, 40, 60 and 80 seconds, respectively. The samples are characterized by LEO1530 Scanning Electron Microscope and XL30 Environmental Scanning Electron Microscope.

3. RESULTS AND DISCUSSION

The mechanism of the TLES is attributed to electrohydrodynamic instabilities. This phenomenon is well characterized for parallel-plate electrode setup under a high electrical field with no thermal gradient for thin polymer liquid films.^{18,19} The primary reason for the formation of pillars has been attributed to periodic fluctuation induced by high electrical field on the free surface.²⁰ Due to the

edge effect, the charges density at the crests of the conical spikes is much higher than that of other areas, thus liquid around the spikes moves to the crests and spikes grow upwards gradually to reach the ground electrode to become pillars, which bridge the anode and the ground cathode. As shown in Figure 2, when the voltage of 160 V was applied to 1.1 μm -thick and 432 nm-thick photoresist 1805 in the electrode gap of 4 μm and 1.1 μm respectively, most of the spikes grew enough to form pillars and protruded from 1805 free surface on silicon substrate with top diameter about several microns to the ground cathode. Similarly, if a high voltage is applied to the thin PEO solution layer in TLES, perturbation is induced on the free surface by interfacial charges. When the electric field is enough, the electric force on the surface overcome the surface tension, gravity and atmospheric pressure, perturbation will be enlarged to become Taylor cone and jet will issue quickly from the top of it to produce nanofibers instead of pillars because the electrode-to-substrate distance is about two order higher than the thickness of PEO solution.

It is very difficult to estimate the exact number of polymer jets. We characterize the yield of electrospun nanofibers by measuring the weight the nanofibers deposited on the collector. For example, for a 3 cm in diameter, 12 cm in length, cylindrical electrode with a setup of electrode-to-substrate distance (the closest distance from

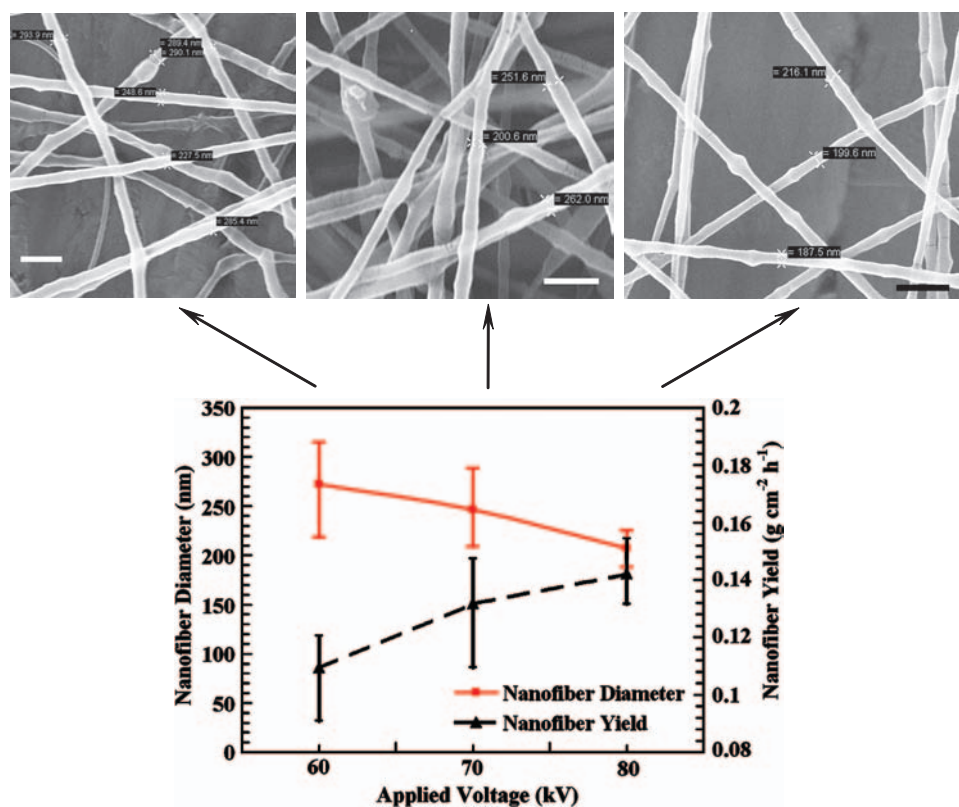


Fig. 3. Yield and diameter of nanofibers versus applied bias voltage. SEM photos of nanofibers on left, center and right are results from applied voltages of 60, 70 and 80 kV respectively. Electrode-to-substrate distance, thickness of thin film, diameter of the cylindrical electrode and PEO concentration are 15 cm, 0.5 mm, 3 cm and 15 wt%, respectively. Scale bar: 1 μm .

the cylindrical electrode to the collector or “H” in Fig. 1(a) at 15 cm, applied voltage at 70 kV, PEO film thickness of 0.5 mm, and polymer solution concentration at 15 wt%, the nanofiber production rate is about $0.13 \text{ g} \cdot \text{cm}^{-2} \cdot \text{h}^{-1}$ or about $5.2 \text{ g} \cdot \text{h}^{-1}$. This is about 260 times higher than that of a traditional, single needle process at a rate of $0.02 \text{ g} \cdot \text{h}^{-1}$.¹⁴ The production rate of nanofibers can be further increased by increasing the applied voltage as shown in Figure 3. As the applied voltage goes up from 60 to 80 kV, the production rate increases from 0.11 to $0.15 \text{ g} \cdot \text{cm}^{-2} \cdot \text{h}^{-1}$. The main reason is believed to be that higher voltage produced stronger instability on the polymer solution and more jets are emerged from the surface of the thin-liquid layer. At the same time, average diameter of nanofiber decreases from 273 nm to 207 nm because more positive charges per unit volume are stored in the liquid jets and stronger electric field induces stronger electric forces to stretch the liquid jets to produce slimmer nanofibers.

It is noted that the bases of liquid jets move randomly during the process with a speed of $0.3 \sim 1 \text{ mm} \cdot \text{s}^{-1}$ in favor of high electrical field areas. For example, artificial tips (base diameter 3 mm and height of 5 mm) made of precision machining process on the surface of the cylindrical electrode attract liquid jets. It is also observed that the base size of the Taylor cone decreases during the electrospinning process as the polymer film thickness decreases. For

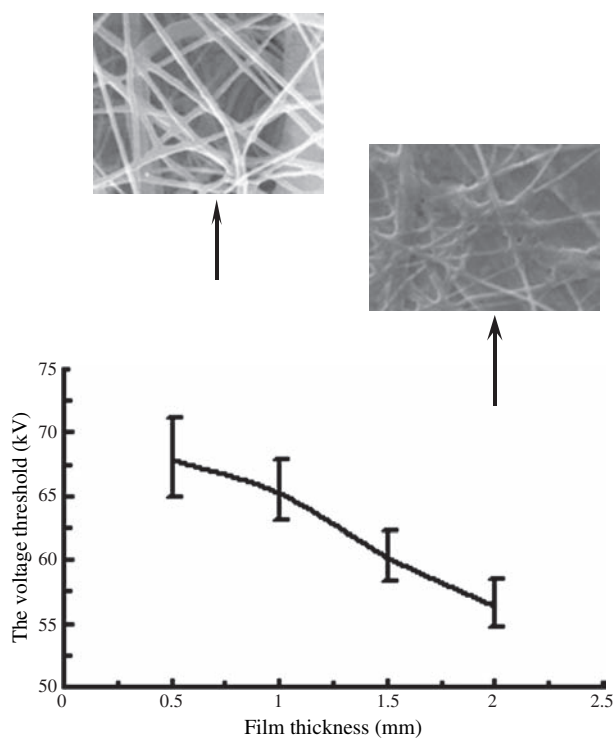


Fig. 4. Threshold voltage versus polymer film thickness. Two SEM images on the top side are TLES results with 0.5 (left) and 2 mm (right) in thickness polymer solutions, respectively. The reference experimental conditions are film thickness of 1 mm, electrode-to-substrate distance of 15 cm and polymer solution of 15 wt%.

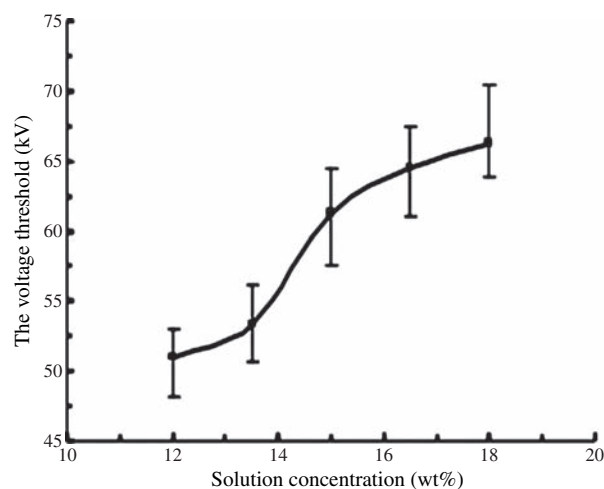


Fig. 5. Experimental results showing threshold voltage versus polymer solution concentrations. The reference experimental conditions are film thickness of 1 mm, electrode-to-substrate distance of 15 cm and polymer solution of 15 wt%.

example, one experiment shows that under initial polymer film thickness of 1 mm, electrode-to-substrate distance of 15 cm, polymer solution of 15 wt%, and applied voltage of 70 kV, the base diameter of the Taylor cone changes from 1.2 to 0.3 mm at the end of the process of about three to four minutes. If the film thickness is further reduced, no Taylor cone or nanofibers can be generated. Studies on the influence of the film thickness with respect to threshold voltage are recorded in Figure 4. When the film thickness increases from 0.5 to 2 mm, the threshold voltage to start TLES reduces from 68 to 56.5 kV. This can be qualitatively explained that thin film with larger thickness is in favor of producing larger Taylor cones to emit nanofibers. The morphology of electrospun nanofibers are also examined using scanning electron microscope (SEM) as shown. It is observed that higher voltage is preferred to produce high quality nanofibers with less clogging effects.

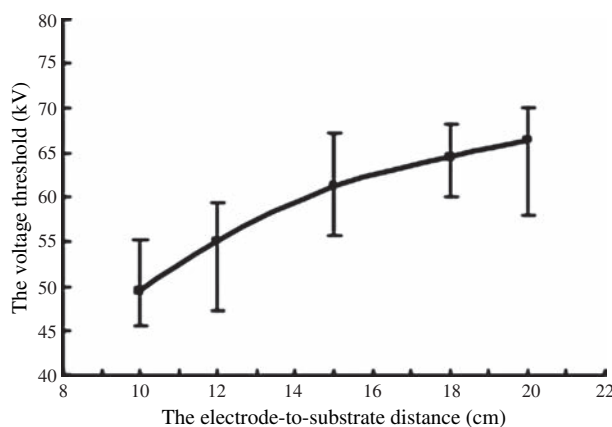


Fig. 6. Results of threshold voltage versus electrode-to-collector distance. The reference experimental conditions are film thickness of 1 mm, electrode-to-substrate distance of 15 cm and polymer solution of 15 wt%.

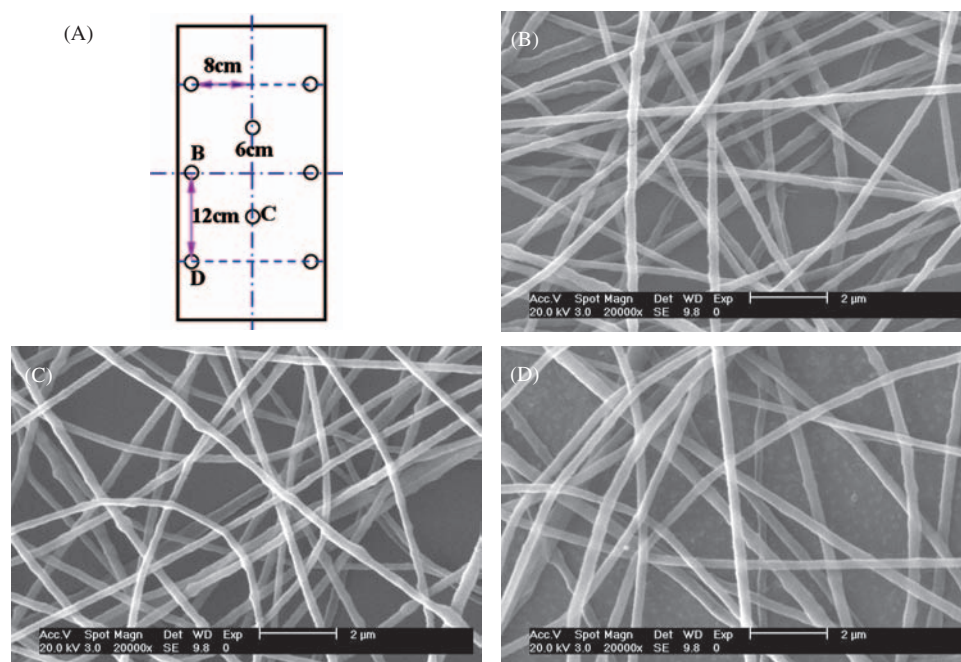


Fig. 7. SEM of nanofibers on the different area of the collector: (A) Schematic diagram of a collector with size of $200 \times 400 \text{ mm}^2$; (B), (C) and (D) are SEM of nanofibers at corresponding areas marked in (A). The applied voltage, the electrode-to-collector distance and the diameter of copper electrode are 70 kV, 150 mm and 30 mm respectively.

Several experiments have been conducted to characterize TLES, including polymer concentration, electrode-to-collector distance, threshold voltage and electrode diameter. The base-line reference conditions include: film thickness of 1 mm, electrode-to-substrate distance of 15 cm, and polymer solution of 15 wt%. Figure 5 shows results of different concentrations (12, 13.5, 15 and 18 wt%) with respect to the threshold voltage. It is found that the applied voltage threshold increases when PEO concentration increases as the viscosity of the solution increases. When the polymer solution concentration is lower than 13.5 wt%, electrospun fibers don't have uniform diameters while higher concentration leads to more stable and uniform deposition of $100 \sim 500 \text{ nm}$ in diameter. Furthermore, in order for nanofibers to solidify thoroughly before touching the collector, it is found that the minimum electrode-to-substrate distance is 10 cm when humidity and temperature are 43% RH and 22° respectively. The effect of the electrode-to-substrate distance on the voltage threshold is studied by changing the distance from 10 to 20 cm as shown in Figure 6. Because the electrical field is proportional to that of the inverse of distance, the threshold voltage increases from 48 to 65 kV when the distance increases from 10 to 20 cm. As the electrode-to-substrate distance increases from 10 to 18 cm, the mean diameter of electrospun nanofibers decreases from 453 nm to 263 nm. When electrode diameter is varied from 1 cm to 6 cm, because to the same bias voltage the electric field intensity decreases with the electrode diameter increasing, experiment results indicate that the threshold voltage increases from about 25 kV to 61 kV. To the applied bias voltage of 70 kV, the

mean diameters of the collected nanofibers from cylindrical electrode diameters of 1–6 cm are all about 200 nm.

In order to achieve more uniform deposition on the collector, the effect of the size of the collector is also investigated on collectors of different sizes of 60×120 , 120×120 , 200×200 and $200 \times 400 \text{ mm}^2$. Experimental results (under 70 kV applied voltage, electrode-to-collector distance of 150 mm, copper electrode of 30 mm in diameter and 12 cm in length, for a 3-min deposition) show that majority of nanofibers are deposited around the edge of the collector for collector size of $60 \times 120 \text{ mm}^2$. Larger size collectors result in more uniform distribution on the collector surface. For example, Figure 7(A) is the schematic view of a collector with size of $200 \times 400 \text{ mm}^2$. Nanofiber deposition results at the left-center edge (marked as B in the Fig. 7(A)), center area (marked as C in the Fig. 7(A)) and left-bottom edge (marked as D in Fig. 7(A)) are illustrated in Figures 7(B), (C) and (D), respectively. It is found that the density of deposited nanofibers is relatively uniform in these areas while slightly higher density can be observed in the edge areas. The primary reason has to do with the edge effects of the electrical field. As the size of the electrode increases, the overall edge effects are reduced.

4. CONCLUSIONS

TLES is a simple method to produce high throughput electrospun nanofibers. Several benefits can be achieved when compared with various multi-jets approach. First, Coulombic interactions between different electrodes are

not present as a single electrode is used. Second, there is no need to control the polymer solution flow rate with pumps as no needles are used. However, the current setup requires cleaning of the polymer solution after each usage and the deposition process stops when the polymer film thickness is reduced to below the threshold value. Furthermore, the film thickness changes during the process and affects the uniformity of the size of nanofibers. One possible solution is to rotate the cylindrical electrode with continuous supply of polymer solution from a bottom reservoir and use a fixed scraper to control the film thickness continuously.

Acknowledgments: This project was supported by National Natural Science Foundation of China (50875222), 863 Program (2007AA04Z308), Program for New Century Excellent Talents of Xiamen University and Innovation Foundation of Xiamen University (No. XDKJCX20063016). We thank Ji Yang for taking excellent optical photos of jet and nanofibers.

References and Notes

1. R. Gopal, S. Kaur, C. Y. Feng, C. Chan, S. Ramakrishna, S. Tabe, and T. Matsuura, *J. Membr. Sci.* 289, 210 (2007).
2. R. Murugan, Z. M. Huang, F. Yang, and S. Ramakrishna, *J. Nanosci. Nanotechnol.* 7, 4595 (2007).
3. S. Lee and S. K. Obendorf, *Text. Res. J.* 77, 696 (2007).
4. M. Tian, Y. Gao, Y. Liu, Y. L. Liao, R. W. Xu, N. E. Hedin, and H. Fong, *Polymer* 48, 2720 (2007).
5. H. Q. Liu, J. Kameoka, D. A. Czaplewski, and H. G. Craighead, *Nano Lett.* 4, 671 (2004).
6. D. Li, Y. L. Wang, and Y. N. Xia, *Adv. Mater.* 16, 361 (2004).
7. A. Theron, E. Zussman, and A. L. Yarin, *Nanotechnology*, 12, 384 (2001).
8. D. H. Sun, C. Chang, S. Li, and L. W. Lin, *Nano Lett.* 6, 839 (2006).
9. C. Chang, K. Limkarilassiri, and L. W. Lin, *Appl. Phys. Lett.* 93, 123111 (2008).
10. W. Tomaszewski and M. Szadkowski, *Fibres Text. East. Eur.* 13, 22 (2005).
11. Y. Y. Zhu, X. X. Wang, D. Z. Wu, and D. H. Sun, *Proc. Int. Conf. Integr. Commer. Micro Nanosyst.* vB, 1169 (2007).
12. G. H. Kim, Y. S. Cho, and W. D. Kim, *Eur. Polym. J.* 42, 2031 (2006).
13. A. L. Yarin and E. Zussman, *Polymer* 45, 2977 (2004).
14. O. O. Dosunmu, G. G. Chase, W. Kataphinan, and D. H. Reneker, *Nanotechnology* 17, 1123 (2006).
15. A. Theron, E. Zussman, and A. L. Yarin, *Polymer* 45, 2017 (2004).
16. H. Fong, I. Chun, and D. H. Reneker, *Polymer* 40, 4585 (1999).
17. G. I. Taylor, *Proc. R. Soc. London Ser. A* 313, 453 (1969).
18. E. Schaffer, T. T. Albrecht, T. P. Russell, and U. Steiner, *Eur. Phys. Lett.* 53, 518 (2001).
19. M. D. Dickey, E. Collister, A. Raines, P. Tsiartas, T. Holcombe, S. V. Sreenivasan, R. T. Bonnecaze, and C. G. Willson, *Chem. Mater.* 18, 2043 (2006).
20. J. Peng, Y. C. Han, Y. M. Yang, and B. Y. Li, *Polymer* 44, 2379 (2003).

Received: 25 May 2009. Accepted: 1 July 2009.